ELSEVIER

Journal of Computational and Applied Mathematics 72 (1996) 193–214

JOURNAL OF COMPUTATIONAL AND APPLIED MATHEMATICS

Ideal free streamline flow over a curved obstacle

J. Hureau*, E. Brunon, Ph. Legallais

E.S.E.M. Laboratoire de Mécanique et Energétique, Rue Leonard de Vinci, 45072 Orleans Cedex 2, France

Received 3 January 1995; revised 10 November 1995

Abstract

In the classical two-dimensional model the description of Helmholtz's (Kirchhoff) flow is a problem of complex analysis which can be solved analytically only for a few simple bodies or polygonal contours, using the Schwarz–Christoffel map. This paper presents a practical method for computing flows over arbitrary obstacles whose boundaries may be piecewise smooth curves, while the impinging flow may be an unbounded flow, a jet, or a semi-infinite stream, i.e. the ocean.

Keywords: Helmholtz (Kirchhoff)'s flow; Free-streamline; Conformal mapping; Jet; Ocean; Wake; Cavity; Curved obstacle; Schwarz–Villat

AMS classification: primary 76B10; secondary 65E05; 30C30

1. Introduction

Usually, in books analyzing the classical theory of the two-dimensional irrotational flow of an ideal incompressible fluid , d'Alembert's paradox is explained by the hypothesis of the ideal fluid. This explanation is not sufficient though, since drag will appear even in an ideal fluid, if the stream flows past an obstacle with a jet break-away, creating a discontinuity in the velocity field.

Helmholtz noticed this in 1868 (and Kirchhoff in 1869), and this led him to the concept of the wake that bears his name: a "dead zone" extending indefinitely behind the obstacle with constant pressure. At the beginning of the century, Levi-Civita [12] and Villat [15] developed the mathematical foundations of the theory underlying this phenomenon. Unfortunately, the velocity field and the free streamlines could be determined only for extremely simple cases. However, it is possible to reverse the problem: given a certain wake, Villat's function can be used to calculate the

* Corresponding author.

SSDI 0377-0427(95)00272-3

obstacle that created it. Later, Leray [13] proved the existence of the solution for any kind of arc and showed the uniqueness for certain types of obstacles [7]. Then, other authors established proofs of uniqueness [2, 9] for further geometries. During this period, Brodetski and Schmieden studied the flow past a circular cylinder. Then many authors, including Riabouchinsky [14], Demtchenko [5], and Chaplygin, extended this theory and applied it to similar flows (with a mirror-plate, an additional wall, a free surface, or a dead zone in front of the obstacle).

The theory then fell into disuse for some time, because the drag coefficients C_D as calculated this way were too small. Only symmetrical patterns and inclined plates could be treated. At the beginning of the 1950s, Birkhoff and Zarantonello [2] used computers to study cylinders; then Wu [16] obtained results for arcs and for a plate with a flap. The monographs of Birkhoff and Zarantonello [2], Jacob [9], Gurevich [7], and Wu [16], give a complete account of various problems concerning jets, wakes and cavities. Lastly, Elcrat and Trefethen [6], using a numerical treatment of the modified Schwarz–Christoffel integral, studied polygonal bodies and other bodies with walls approximated by polygonal lines. To our knowledge, the problem of flows with Helmholtz wakes caused by an obstacle in an unbounded flow has never been solved as of today for any curved walls except circular and elliptic arcs.

Following previous studies [8], this paper presents a method for solving this problem in the case of an unbounded stream (Helmholtz's flow). The scheme will then be extended to determine the flow around any obstacle, first in a jet, and then in an ocean (the former being the more complex situation) (Fig. 1). For each type of flow, we shall test the accuracy of our results by comparison with those previously published [1, 2, 4, 6], and then compute the free streamlines and the values of C_D and C_L for various contours.

2. Obstacle in an unbounded flow

An obstacle of known geometry is placed in an infinite stream of velocity V_∞, parallel to the x-axis, and of pressure P_∞. $\mathscr{P}$ is the wetted wall, A is the upstream infinite located point, and D is the stagnation point. C and E are the points where the flow separates from $\mathscr{P}$, and $\mathscr{L}_{CB}$ and $\mathscr{L}_{EF}$ are the free streamlines coming from C and E (Fig. 2(a)).

Let $f(z)$ be the complex potential and its derivative $w(z)$ the complex velocity.

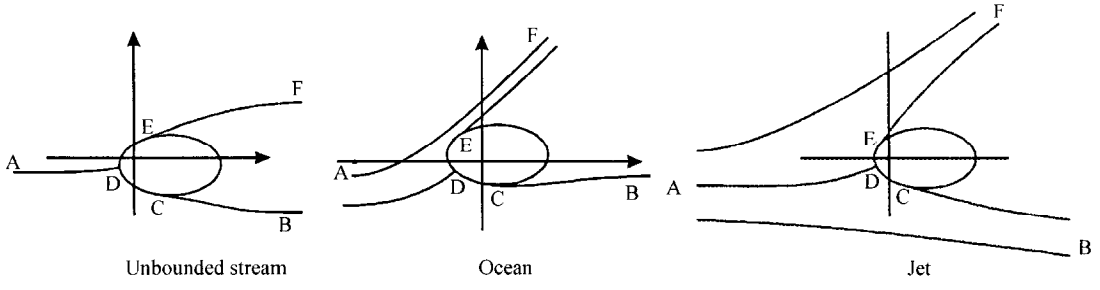

Fig. 1.

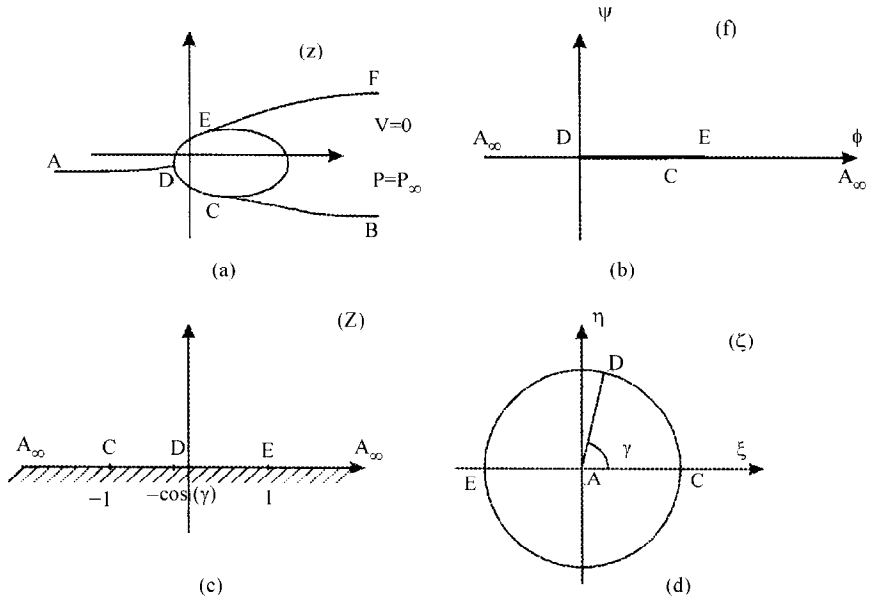

Fig. 2.

The boundary conditions are:

$$\lim_{z\to\infty} w(z) = V_\infty, \tag{1}$$

$$\mathrm{Im}\{w(z)\,\mathrm{d}z\} = 0 \quad \text{on } \mathscr{P}, \tag{2}$$

$$|w(z)| = V_\infty \quad \text{on } \mathscr{L}_{CB} \text{ and } \mathscr{L}_{EF}. \tag{3}$$

The locations of points C and E used to be obtained by Brillouin's conditions [3]. The first of these conditions assumes that the pressure is minimum in the "dead zone". Actually this is true only in cavitational flows. According to the second condition, the curvature of the free streamlines $\mathscr{L}_{CB}$ and $\mathscr{L}_{EF}$ at C and E is finite. These conditions were used to obtain equations to calculate the positions of points C and E. In fact, only by analyzing the boundary layer can we calculate the location of the current break-away points. We shall therefore assume that points C and E are always specified.

2.1. Levi-Civita and Villat method

Here, the problem is not solved by calculating f or w, but rather by determining the function Ω defined by the following relations:

$$w = V_\infty \mathrm{e}^{-\mathrm{i}\Omega}, \tag{4}$$

$$\Omega = \Theta + \mathrm{i}T, \tag{5}$$

where Θ is the angle the fluid velocity makes with the x-axis, and T is given by

$$|\vec{V}| = V_\infty e^T.$$

This is a mixed problem for Ω, because Θ is known on $\mathscr{P}$, and $T = 0$ on $\mathscr{L}_{CB}$ and $\mathscr{L}_{EF}$.

The Levi-Civita method consists in mapping the f-plane on the inside of the upper unit semi-circle, named Δ^+, in such a way that the free streamlines map onto the diameter. Since $T = 0$ on the diameter, the function can then, according to Schwarz's principle of symmetry, be continued inside the circle, named Δ. The mixed problem then becomes a Dirichlet problem and we use the Schwarz–Villat formula to determine Ω and, consequently, $\tau(\sigma) = T(e^{i\sigma})$, if we know $\theta(\sigma) = \Theta(e^{i\sigma})$ on the circular boundary of Δ.

The diagrams in the different planes used are shown in Fig. 2.

In the f-plane let $\mathscr{D}$ be the domain corresponding to the flow domain in the z-plane.

The following classical transformations are used to map $\mathscr{D}$ on Δ^+ in the ζ-plane:

$$f = a^2(Z + \cos(\gamma))^2, \tag{6}$$

$$Z = -\tfrac{1}{2}\left(\zeta + \frac{1}{\zeta}\right), \tag{7}$$

with

$$a = \frac{\sqrt{\varphi_E} + \sqrt{\varphi_C}}{2} \quad \text{and} \quad \cos(\gamma) = \frac{\sqrt{\varphi_E} - \sqrt{\varphi_C}}{\sqrt{\varphi_E} + \sqrt{\varphi_C}},$$

where φ_C and φ_E are the velocity potential values at C and E, and the value $\zeta = e^{i\gamma}$ corresponds to point D.

From (6) and (7), we obtain

$$f = a^2\left[\cos(\gamma) - \tfrac{1}{2}\left(\zeta + \frac{1}{\zeta}\right)\right]^2. \tag{8}$$

Since φ_C and φ_E are unknown, a and γ are constants to be determined.

Eq. (3) implies $T = 0$ for $\zeta \in [-1, 1]$. Ω can consequently be extended to an analytic function, regular inside the unit circle $|\zeta| < 1$. From (1), $\Omega(0) = 0$, so the constant of the Schwarz–Villat formula is null and the function Ω is easily calculated knowing $\theta(\sigma)$ (Villat's function):

$$\Omega(\zeta) = \frac{1}{\pi}\int_0^\pi \frac{1 - \zeta^2}{1 - 2\zeta\cos(\sigma) + \zeta^2}\,\theta(\sigma)\,d\sigma, \tag{9}$$

$dz = df/w$ used with (4) and (8) gives

$$dz = \frac{K}{4}e^{i\Omega}\left[\left(\zeta + \frac{1}{\zeta}\right) - 2\cos(\gamma)\right]\left[1 - \frac{1}{\zeta^2}\right]d\zeta, \tag{10}$$

where $K = 2a^2/V_\infty$.

The parametric equations of the free streamlines $\mathscr{L}_{CB}$ and $\mathscr{L}_{EF}$ are obtained by integrating (10) from $\zeta = \pm 1$ to ζ', where ζ' is a point on AC or EA. On the boundary of Δ, $\zeta = e^{i\sigma}$ and (10) becomes

$$dz = Ke^{i\theta}e^{-\tau}(\cos(\gamma) - \cos(\sigma))\sin(\sigma)\,d\sigma. \tag{11}$$

Let s be the arc length of z onto $\mathscr{P}$ starting from C, $s \in [0, L]$ (L is the length of $\mathscr{P}$).

$$ds = Ke^{-\tau}(\cos(\gamma) - \cos(\sigma))\sin(\sigma)\,d\sigma. \tag{12}$$

This looks easy to solve, but the fact that the $\theta(\sigma)$ function used in (9) is unknown must be emphasized. This is why the first problems treated had very simple $\theta(\sigma)$ functions, such as two-value function for a flat plate or a wedge. Later, we were able to treat cylinders by introducing the curvature of $\mathscr{P}$ in a formula replacing (12), but other kinds of obstacles cannot be studied directly: Curved walls must be approximated by a polygonal line [6], or the problem must be reversed, by prescribing $\theta(\sigma)$ so that the corresponding obstacle can be determined.

2.2. *The functional system*

The singularity of Ω at the stagnation point is isolated by expressing:

$$\Omega = \Omega_S + \tilde{\Omega}, \tag{13}$$

where Ω_S is a particular solution having the same singularity of Ω.

$$\Omega_S = \theta_S + i\tau_S = -\frac{3\pi}{2} + \gamma + i\log\left(\frac{e^{i\sigma} - e^{i\gamma}}{e^{i\sigma} - e^{-i\gamma}}\right),$$

$$\theta_S = -\frac{\pi}{2} \quad \text{for } \sigma \in [0, \gamma[,$$

$$\theta_S = \frac{\pi}{2} \quad \text{for } \sigma \in]\gamma, \pi],$$

$$\tau_S = \ln\left|\frac{\sin((\sigma-\gamma)/2)}{\sin((\sigma+\gamma)/2)}\right| \Rightarrow e^{\tau} = e^{\tilde{\tau}}\left|\frac{\sin((\sigma-\gamma)/2)}{\sin((\sigma+\gamma)/2)}\right|.$$

As Ω_S is known, we must analyze $\tilde{\Omega} = \tilde{\theta} + i\tilde{\tau}$.

Let β be the angle between the tangent at a point on $\mathscr{P}$ and the x-axis, and ε the one-to-one boundary correspondence function:

$$\varepsilon: \quad \sigma \in [0, \pi] \rightarrow s \in [0, L]. \tag{14}$$

Eq. (12) can then be written as

$$\varepsilon(\sigma) = K\int_0^{\sigma} \frac{2\sin(\sigma')\sin^2((\sigma'+\gamma)/2)}{e^{\tilde{\tau}(\sigma')}}\,d\sigma'. \tag{15}$$

Then, from the geometry of the contour, let us write:

$$\tilde{\theta}(\sigma) = (\beta \circ \varepsilon)(\sigma) - \frac{\pi}{2} \quad \forall \sigma \in [0, \pi], \tag{16}$$

$\tilde{\tau}$ is calculated using Schwarz–Villat's formula:

$$\tilde{\tau}(\sigma) = \frac{1}{\pi} \lim_{\zeta \to e^{i\sigma}} \operatorname{Im} \left\{ \int_0^{\pi} \frac{1 - \zeta^2}{1 - 2\zeta \cos(\sigma') + \zeta^2} \tilde{\theta}(\sigma') \, d\sigma' \right\}. \tag{17}$$

$\Omega(0) = 0$ means $\int_0^{\pi} \theta(\sigma') \, d\sigma' = 0$, hence,

$$\gamma = \frac{\pi}{2} + \frac{1}{\pi} \int_0^{\pi} \tilde{\theta}(\sigma') \, d\sigma', \tag{18}$$

$\varepsilon(\pi) = L$ allows us to determine K, and we write [15] in the form

$$\varepsilon(\sigma) = L\left(\frac{E(\sigma, \gamma)}{E(\pi, \gamma)}\right), \quad \text{where } E(\sigma, \gamma) = \int_0^{\sigma} \frac{2 \sin(\sigma') \sin^2((\sigma' + \gamma)/2)}{e^{\tilde{\tau}(\sigma')}} \, d\sigma'. \tag{19}$$

The unknowns are the functions $\sigma \to \tilde{\theta}$, $\tilde{\tau}$, ε and the angle γ.

Relations (16)–(19) supply a functional system of four equations written as

$$\tilde{\theta} = \mathscr{I}(\varepsilon), \tag{16'}$$

$$\tilde{\tau} = \mathscr{L}(\tilde{\theta}), \tag{17'}$$

$$\gamma = \mathscr{D}(\tilde{\theta}), \tag{18'}$$

$$\varepsilon = \mathscr{E}(\tilde{\tau}, \gamma). \tag{19'}$$

2.3. Numerical procedure

Let us define four weighting factor $r_\theta, r_\gamma, r_\tau, r_\varepsilon$ belonging to $[0, 1]$. From any initial correspondence function ε_0, we build a series $\tilde{\theta}_n, \gamma_n, \tilde{\tau}_n, \varepsilon_n$, using the following recursive algorithm:

$$\tilde{\theta}_n = (1 - r_\theta) \mathscr{I}(\varepsilon_{n-1}) + r_\theta \tilde{\theta}_{n-1},$$

$$\gamma_n = (1 - r_\gamma) \mathscr{D}(\tilde{\theta}_{n-1}) + r_\gamma \gamma_{n-1},$$

$$\tilde{\tau}_n = (1 - r_\tau) \mathscr{L}(\tilde{\theta}_{n-1}) + r_\tau \tilde{\tau}_{n-1},$$

$$\varepsilon_n = (1 - r_\varepsilon) \mathscr{E}(\tilde{\tau}_{n-1}, \gamma_{n-1}) + r_\varepsilon \varepsilon_{n-1}.$$

The integrals of (17) and (18) are approximated by a quadrature method based on a regular subdivision of $[0, \pi]$. The existence and uniqueness of the solution has been proved. If the process converges, the solution is reached, then the process is stopped by a test on the relative error associated with some unknown (usually ε).

After convergence, it is easy to calculate w and thus find the pressure distribution, the drag, and the lift. These values will be compared to those obtained using Blasius's theorem:

$$R_x = \frac{\rho \pi K V_\infty^2}{8} \Omega'^2(0),$$

$$R_y = \frac{\rho \pi K V_\infty^2}{8} [4 \cos(\gamma) \Omega'(0) - \Omega''(0)].$$

In most cases, the number of iterations varies from 10 to 50, corresponding to a few minutes' calculations on a PC 486-DX 50-type computer. The accuracy can be improved by increasing the number of iterations and quadrature points (usually 500 points).

The weighting factors may be zero. To study obstacles with high curvature, we will use $r_\varepsilon = r_\theta = r_\tau = 0.5$ and $r_\gamma = 0$ to obtain convergence. For polygonal obstacles, the weighting factors must be greater.

3. Extension of the method

Since we have studied an obstacle in an infinite stream. Extending the method means considering an obstacle in a jet, and then in an ocean (semi-infinite stream).

3.1. Jet impinging an obstacle

Let a jet of finite width h_∞, of velocity V_∞ parallel to the x-axis, and of pressure P_∞, be divided by a body of given geometry. The pressure of the motionless fluid is also P_∞. A is the point at infinity on the impinging jet, D is the stagnation point, $\mathscr{P}$ is the wetted wall, and E and C are the separation points. On the obstacle, the impinging jet divides into two jets bounded by the free streamlines $\mathscr{L}_{AB}$, $\mathscr{L}_{CB}$ and $\mathscr{L}_{EF}$, $\mathscr{L}_{AF}$. At infinity, they make angles α_B and α_F with the x-axis, and their widths are h_B and h_F. The position of the contour in the z-plane and the H level of the upstream jet axis are known (Fig. 3(a)).

The diagrams in the different planes used are shown in Fig. 3.

In the f-plane let $\mathscr{D}$ be the domain corresponding to the flow domain in the z-plane.

The boundary conditions are:

$$\lim_{z\to A} w(z) = V_\infty, \tag{20}$$

$$\operatorname{Im}\{w(z)\,dz\} = 0 \quad \text{on } \mathscr{P}, \tag{21}$$

$$|w(z)| = V_\infty \quad \text{on } \mathscr{L}_{AB}\cup\mathscr{L}_{CB}\cup\mathscr{L}_{EF}\cup\mathscr{L}_{AF}. \tag{22}$$

Now there are two additional conditions:

$$\lim_{z\to F} w(z) = V_\infty e^{-i\alpha_F}, \tag{23}$$

$$\lim_{z\to B} w(z) = V_\infty e^{-i\alpha_B}, \tag{24}$$

As in Section 2 we solve by determining $\Omega = \Theta + iT$. Θ is known on $\mathscr{P}$, and T is zero on the free streamlines $\mathscr{L}_{AB}$, $\mathscr{L}_{CB}$, $\mathscr{L}_{EF}$ and $\mathscr{L}_{AF}$. Levi-Civita's method reduces the mixed problem to a Dirichlet problem. Hence, we must map the f-plane on the ζ-plane.

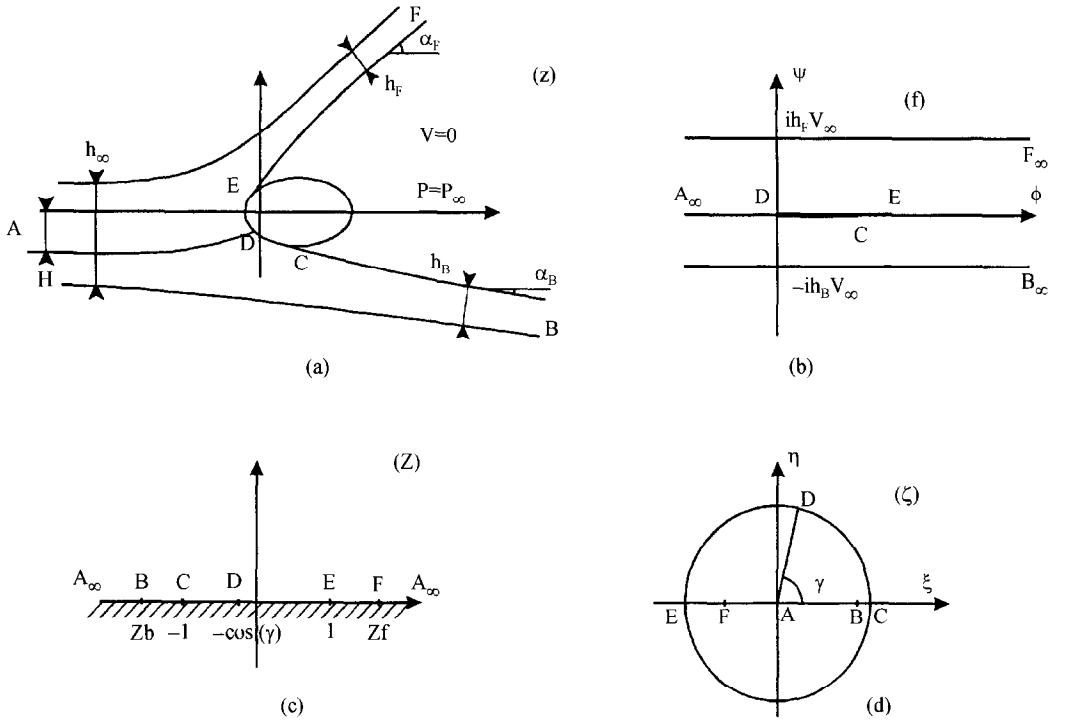

Fig. 3.

The successive conformal maps are:

$$f = -\frac{V_\infty h_B}{\pi}\log(Z - Z_B) - \frac{V_\infty h_F}{\pi}\log(Z - Z_F) + \text{Const.}, \tag{25}$$

where

$$\frac{h_F}{h_B} = -\frac{Z_F + \cos(\gamma)}{Z_B + \cos(\gamma)},$$

$$Z = -\tfrac{1}{2}\left(\zeta + \frac{1}{\zeta}\right). \tag{26}$$

The function mapping $\mathscr{D}$ onto Δ^+ is

$$f = -\frac{V_\infty h_B}{\pi}\log\left(-\frac{1}{2}\left(\zeta + \frac{1}{\zeta}\right) - Z_B\right) - \frac{V_\infty h_F}{\pi}\log\left(-\frac{1}{2}\left(\zeta + \frac{1}{\zeta}\right) - Z_F\right) + \text{Const.} \tag{27}$$

Z_B, Z_F, h_B and h_F being unknown.

From (20), $\Omega(0) = 0$, so Schwarz–Villat's formula gives function Ω knowing $\theta(\sigma)$ (Villat's function), and $dz = df/w$ used with (27) gives

$$dz = \frac{e^{i\theta}}{\pi e^{\tau}}\left[\frac{h_B}{\left(\zeta + \frac{1}{\zeta}\right) + 2Z_B} + \frac{h_F}{\left(\zeta + \frac{1}{\zeta}\right) + 2Z_F}\right]\left(\frac{1-\zeta^2}{\zeta^2}\right)d\zeta. \tag{28}$$

Now the parametric equations of the free streamlines can be calculated with $\zeta \in [-1, 1]$. On the circle $\zeta = e^{i\sigma}$ and (28) becomes

$$dz = \frac{e^{i\theta}}{\pi e^{\tau}}\left[\frac{h_B}{\cos(\sigma) + Z_B} + \frac{h_F}{\cos(\sigma) + Z_F}\right]\sin(\sigma)\,d\sigma, \tag{29}$$

hence, the arc length s is given by

$$ds = \frac{1}{\pi e^{\tau}}\left[\frac{h_B}{\cos(\sigma) + Z_B} + \frac{h_F}{\cos(\sigma) + Z_F}\right]\sin(\sigma)\,d\sigma, \tag{30}$$

The singularity of Ω at the stagnation point is the same as in Section 2, so τ_S and θ_S remain unchanged and we have $\tilde{\Omega} = \tilde{\theta} + i\tilde{\tau}$ to analyze.

We use Ω_S, h_F/h_B (as described above), (25), and the conservation of mass to define the one-to-one boundary correspondence function $\varepsilon(\sigma)$ by writing (30) as

$$\varepsilon(\sigma) = -\frac{2h_\infty}{\pi}\int_0^\sigma \frac{1}{e^{\tilde{\tau}}}\frac{\sin(\sigma')\sin^2((\sigma' + \gamma)/2)}{(\cos(\sigma') + Z_B)(\cos(\sigma') + Z_F)}\,d\sigma'. \tag{31}$$

The geometry of the obstacle leads to

$$\tilde{\theta}(\sigma) = (\beta \circ \varepsilon)(\sigma) - \frac{\pi}{2} \quad \forall \sigma \in [0, \pi], \tag{32}$$

$\tilde{\tau}$ is calculated by means of Schwarz–Villat's formula:

$$\tilde{\tau}(\sigma) = \frac{1}{\pi}\lim_{\zeta \to e^{i\sigma}} \mathrm{Im}\left\{\int_0^\pi \frac{1-\zeta^2}{1 - 2\zeta\cos(\sigma') + \zeta^2}\tilde{\theta}(\sigma')\,d\sigma'\right\}, \tag{33}$$

$\Omega(0) = 0$ means $\int_0^\pi \tilde{\theta}(\sigma')\,d\sigma' = 0$. Hence,

$$\gamma = \frac{\pi}{2} + \frac{1}{\pi}\int_0^\pi \tilde{\theta}(\sigma')\,d\sigma'. \tag{34}$$

There are two unknowns in (31): Z_B and Z_F related to α_B and α_F.

Two additional relations must be written to determine Z_B and Z_F:

- The length of the wetted wall is L, so $\varepsilon(\pi) = L$ which leads to

$$\varepsilon(\sigma) = L\left(\frac{E(\sigma, \gamma)}{E(\pi, \gamma)}\right). \tag{35}$$

where

$$\varepsilon(\sigma,\gamma)=\int_0^{\sigma}\frac{1}{e^{\tilde{\tau}}}\frac{\sin(\sigma')\sin^2((\sigma'+\gamma)/2)}{(\cos(\sigma')+Z_B)(\cos(\sigma')+Z_F)}\,d\sigma'.$$

- From the position of the obstacle with respect to the jet axis, it is possible to write:

$$\operatorname{Im}\left\{z_D+\int_{\mathscr{L}_{AD}}dz\right\}=H+\frac{h_\infty}{2}-h_F, \tag{36}$$

where Z_D is the affix of D and $\mathscr{L}_{AD}$ is the stagnation streamline.

The unknowns are the functions $\sigma\to\tilde{\theta},\tilde{\tau},\varepsilon$, and the angle γ.

Relations (31)–(34) supply a functional system of four equations similar to the system expressed in Section 2. The solution is found in the same way by building a series $\tilde{\theta}_n$, γ_n, $\tilde{\tau}_n$, ε_n using a recursive-type algorithm and an arbitrary initial correspondence function ε_0.

3.2. *Planing on the surface of a stream*

Let us consider the two-dimensional problem of planing on the surface of a fluid occupying the entire lower half plane. After a change of axis, we consider a stationary obstacle impinged by a stream of infinite depth and velocity V_∞ parallel to the x-axis and pressure P_∞. The pressure of the motionless fluid is also P_∞. A is the upstream infinite located point, D the stagnation point, E and C the separation points, and $\mathscr{P}$ the wetted wall. Now a jet bounded by the free streamlines $\mathscr{L}_{EF}$ and $\mathscr{L}_{AF}$ is formed at the leading edge of the obstacle. At infinity it makes an angle α_F with the x-axis and its thickness is h_F. Downstream, the surface of the fluid is the free streamline $\mathscr{L}_{CB}$ (Fig. 4(a)).

This configuration could represent the movement of a finite body along the surface of very deep water, but Birkhoff and Zarantonello [2] and Gurevich [7] showed that, for a weightless and infinitely deep fluid, the obstacle rises infinitely high above the level of the fluid at infinity. Consequently, the obstacle position is known in the z-plane, but the H level of the free surface streamline at infinity upstream of the planing body is not. In order to represent the true motion, the effect of gravity or a finite depth must be taken into account. So the problem of a planing surface is not a special case of the preceding one, but the way we set about solving it is the same.

The diagrams used in the different planes are shown in Fig. 4.

Note that a planing contour can be considered as a submerged hydrofoil whose cavitation number $Q=0$ and whose wetted wall is of finite length. We will not consider this as a special case of an infinite submerged hydrofoil in which point E coincides with point F.

In the f-plane, z-plane and ζ-plane, points A and B are the same, so the boundary conditions are quite similar:

$$\lim_{z\to A\text{ or }B} w(z)=V_\infty, \tag{37}$$

$$\operatorname{Im}\{w(z)\,dz\}=0 \quad \text{on } \mathscr{P}, \tag{38}$$

$$|w(z)|=V_\infty \quad \text{on } \mathscr{L}_{CB}\cup\mathscr{L}_{EF}\cup\mathscr{L}_{AF}, \tag{39}$$

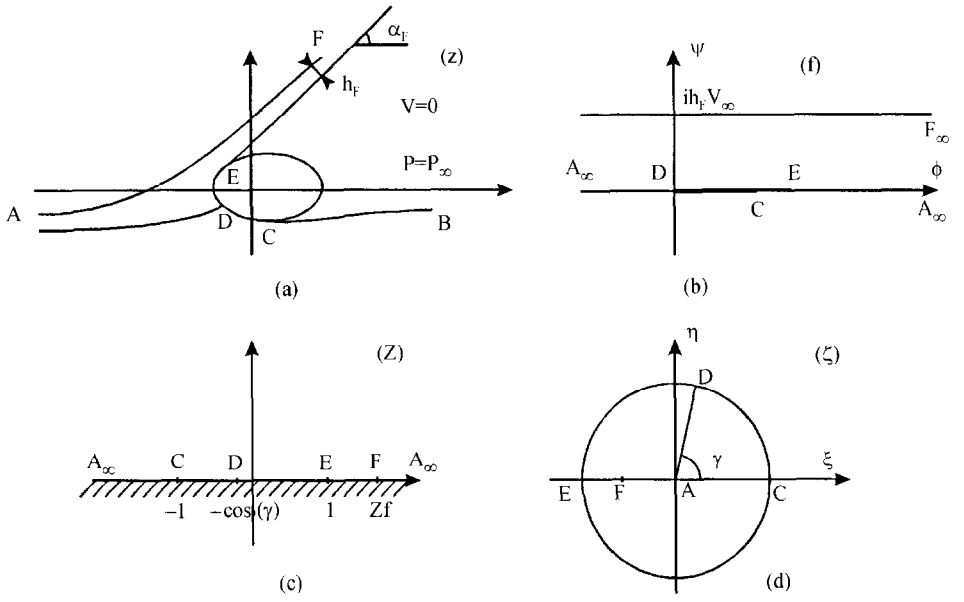

Fig. 4.

to which we add

$$\lim_{z\to F} w(z) = V_\infty e^{-i\alpha_F}. \tag{40}$$

As a matter of fact, $\mathscr{D}$ in the f-plane has been modified so,

$$f = \frac{V_\infty h_F}{\pi(Z_D - Z_F)}(\log(Z - Z_F)(Z_F - Z_D) + (Z - Z_F)) + \text{Const.} \tag{41}$$

By using the same $Z(\zeta)$ transformation as in Section 3.1, the function that maps $\mathscr{D}$ onto Δ^+ is

$$f = \frac{V_\infty h_F}{\pi(Z_D - Z_F)}\left(\log\left(-\frac{1}{2}\left(\zeta + \frac{1}{\zeta}\right) - Z_F\right)(Z_F - Z_D) + \left(-\frac{1}{2}\left(\zeta + \frac{1}{\zeta}\right) - Z_F\right)\right) + \text{Const.} \tag{42}$$

Z_F and h_F being unknown.

Schwarz–Villat's formula and (42) lead to

$$dz = \frac{h_F e^{i\theta}}{\pi e^{\tau}(Z_D - Z_F)}\left[\frac{Z_D - Z_F}{(\zeta + 1/\zeta) + 2Z_F} + \frac{1}{2}\right]\left(\frac{1 - \zeta^2}{\zeta^2}\right)d\zeta, \tag{43}$$

which enables us to write on the circle:

$$dz = \frac{h_F e^{i\theta}}{\pi e^{\tau}(Z_D - Z_F)}\frac{\cos(\sigma) - \cos(\gamma)}{(\cos(\sigma) + Z_F)}\sin(\sigma)\,d\sigma. \tag{44}$$

and the arc length s is calculated with

$$ds = \frac{h_F}{\pi e^{\tau}(Z_D - Z_F)} \frac{\cos(\sigma) - \cos(\gamma)}{(\cos(\sigma) + Z_F)} \sin(\sigma)\, d\sigma. \tag{45}$$

As the stagnation point's singularity is the same as that of the previous section, everything we have said about $\tilde{\Omega}$ and Ω remains unchanged, which leads to the expressions

$$\tilde{\theta}(\sigma) = (\beta \circ \varepsilon)(\sigma) - \frac{\pi}{2} \quad \forall \sigma \in [0, \pi], \tag{46}$$

$$\tilde{\tau}(\sigma) = \frac{1}{\pi} \lim_{\zeta \to e^{i\sigma}} \operatorname{Im} \left\{ \int_0^{\pi} \frac{1 - \zeta^2}{1 - 2\zeta \cos(\sigma') + \zeta^2} \tilde{\theta}(\sigma')\, d\sigma' \right\}, \tag{47}$$

$$\gamma = \frac{\pi}{2} + \frac{1}{\pi} \int_0^{\pi} \tilde{\theta}(\sigma')\, d\sigma' \tag{48}$$

and the one-to-one boundary correspondence function $\varepsilon(\sigma)$ is defined by

$$\varepsilon(\sigma) = \frac{2h_F}{\pi} \int_0^{\sigma} \frac{1}{e^{\tilde{\tau}}} \frac{\sin(\sigma') \sin^2((\sigma' + \gamma)/2)}{(\cos(\sigma') + Z_F)(\cos(\gamma) + Z_F)}\, d\sigma'. \tag{49}$$

There are still two unknowns in $\varepsilon(\sigma)$: h_F, the width of the jet, and Z_F, which is related to α_F.

Now, conservation of mass cannot be used; and, as was said at the beginning of this section, we can express only one additional formula to define $\varepsilon(\sigma)$:

- $\varepsilon(\pi) = L$, which leads to

$$\varepsilon(\sigma) = L\left(\frac{E(\sigma, \gamma)}{E(\pi, \gamma)}\right), \tag{50}$$

where

$$E(\sigma, \gamma) = \int_0^{\sigma} \frac{1}{e^{\tilde{\tau}}} \frac{\sin(\sigma') \sin^2((\sigma' + \gamma)/2)}{(\cos(\sigma') + Z_F)(\cos(\gamma) + Z_F)}\, d\sigma'.$$

The unknowns are the functions $\sigma \to \tilde{\theta}, \tilde{\tau}, \varepsilon$, the angle γ, and Z_F (or h_F).

Relations (46)–(48) and (50) supply a functional system of four equations similar to the one expressed in Section 2. A Z_F value must be chosen to solve by building a series $\tilde{\theta}_n, \gamma_n, \tilde{\tau}_n, \varepsilon_n$ using an algorithm of the recursive type, and any initial correspondence function ε_0. So we compute the velocity distribution and the free streamlines, α_F and h_F for a given geometry of the planing surface. This way, it is quite easy to describe the flow for a given geometry and h_F, by prescribing h_F instead of Z_F.

4. Dealing with boundary singularities

The presence of corners on $\mathscr{P}$ upsets the preceding formulation. Moreover, the positions of corners on the circle are unknown since they depend on the unknown function ε.

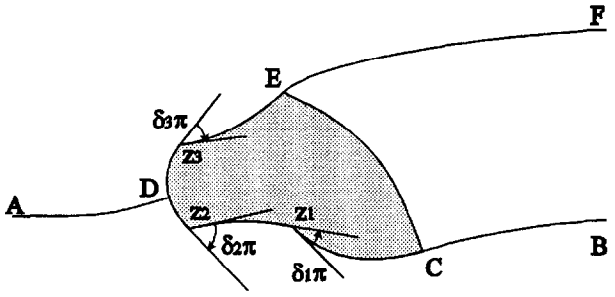

Fig. 5.

Now consider the wetted wall with N corners (Fig. 5). Let z_k $(1 \leqslant k \leqslant N)$ be the affix of one vertex, and $\zeta_k = e^{i\gamma_k}$ its image in the ζ-plane. It is clear that the velocity is discontinuous at this point:

- its argument θ jumps by $\delta_k \pi$,
- its norm is either zero or infinite.

Therefore, Ω has the following singularities:

- its real part jumps by $\delta_k \pi$,
- its imaginary part is infinite.

In Δ we express Ω by means of Schwarz–Villat's formula. Hence, $\theta(\sigma)$ would be continuous. It is necessary to isolate the singularity by writing

$$\Omega = \Omega_S + \tilde{\Omega}, \quad \text{with} \quad \Omega_S = \Omega_D + \Omega_P.$$

Ω_D comes from the stagnation point singularity whereas Ω_P comes from the corner singularities.

To continue Ω into the lower semicircle by the principle of reflexion, Levi-Civita's method requires that $\theta(\sigma) = \theta(2\pi - \sigma)$. This means that the singular part of Ω must be isolated at point ζ_k, and its conjugate $\overline{\zeta}_k = e^{-i\gamma_k}$. A simple function satisfying these conditions is $i\delta_k \log((\zeta - e^{i\gamma_k})/(\zeta - e^{-i\gamma_k}))$.

Hence, the solution for an obstacle having N corners is

$$\Omega_P = i \sum_{k=1}^{k=N} [\log(\zeta - e^{i\gamma_k})^{\delta_k} + \log(\zeta - e^{-i\gamma_k})^{-\delta_k}].$$

This leads us to: $\theta_P = \theta'_P + \theta''_P$, where

$$\theta'_P(\sigma) = \sum -\delta_k(\gamma_k + \pi) \quad \text{for } \gamma_k \in [0, \sigma[,$$

$$\theta''_P(\sigma) = \sum -\delta_k \gamma_k \quad \text{for } \gamma_k \in]0, \pi],$$

And

$$\tau_P(\sigma) = \sum_{k=1}^{k=N} \delta_k \ln \left| \frac{\sin((\sigma - \gamma_k)/2)}{\sin((\sigma + \gamma_k)/2)} \right| \quad \text{on } [0, \pi].$$

In every case we have treated, if the wetted wall of the obstacle has one or several corners, then the Ω_S function which was reduced to Ω_D has to be replaced by $\Omega_S = \Omega_D + \Omega_P$.

Remembering that relations (18), (34) and (48) are obtained from $\Omega(0) = 0$, it is obvious that if function Ω is modified, these expressions must be substituted by

$$\gamma = \frac{\pi}{2} + \frac{1}{\pi}\int_0^{\pi} \tilde{\theta}(\sigma)\,\mathrm{d}\sigma - 2\sum_{k=1}^{k=N} \delta_k \gamma_k.$$

5. Computed results

5.1. Obstacle in an unbounded flow

To test the capacity of our program we compared the C_D and C_L that it computed with the exact values, or values given in the literature. The classical results are those of the inclined flat plate and the circular cylinder. First we consider three obstacles with straight boundaries, then obstacles with curved boundaries.

5.1.1. Inclined plate

This is a geometry whose exact solution is well-known. The classical values of C_D, C_L, and γ are:

$$\gamma = \delta + \frac{\pi}{2}, \qquad C_D = \frac{\pi\cos^2(\delta)}{4 + \pi\cos(\delta)} \quad \text{and} \quad C_L = \frac{\pi\cos(\delta)\sin(\delta)}{4 + \pi\cos(\delta)},$$

where δ is the angle between the perpendicular to the wall and the x-axis.

In Table 1 we give, for different values of δ, the values of C_D, C_L, and γ as obtained from these formulas and the values of $C_{D\mathrm{Helm}}$, $C_{L\mathrm{Helm}}$, and γ_{Helm} we computed. Our program reproduces the exact values of C_D, C_L and γ.

5.1.2. Inclined plate with separation on the backface

Let us consider a plate inclined at an angle of 30° with the separation point prescribed in the middle of the back face. This was studied by Chaplygin and Laurentiev in 1933, and recently by Elcrat and Trefethen [6]. Their computed values of C_D and C_L are:

$$C_D = 0.000575, \qquad C_L = 2.26628.$$

Table 1

δ	C_D	$C_{D\,\mathrm{Helm}}$	C_L	$C_{L\,\mathrm{Helm}}$	γ	γ_{Helm}
0	0.879802	0.879801	0.000000	0.000000	90	90.0
15	0.833358	0.833357	0.223297	0.223297	105	105.0
30	0.701175	0.701175	0.404824	0.404823	120	120.0
45	0.504962	0.504962	0.504962	0.504962	135	135.0
60	0.281970	0.281970	0.488386	0.488386	150	150.0
75	0.087447	0.087447	0.326358	0.326357	165	165.0

Table 2

Φ	15 °	30 °	45 °	60 °	120 °	-22.5 °	-45 °
C_D B – Z	0.81912	0.76288	0.67766	0.57024	0.00766	0.93330	0.96694
C_D Helm	0.82910	0.76284	0.67764	0.57024	0.00765	0.93327	0.96697

We find

$C_D = 0.0005740$, $C_L = 2.26652$ (using 500 quadrature points),

$C_D = 0.0005744$, $C_L = 2.26634$ (using 1100 quadrature points).

The more we increase the number of quadrature points, the more precisely we get the values of Elcrat and Trefethen.

5.1.3. Asymmetrical wedge

The upper face of the wedge is inclined at an angle of 30°, the lower face at 45°, and both faces are the same length. This case was studied by Elcrat and Trefethen [6], who computed

$C_D = 0.33703$, $C_L = 0.07397$.

We find:

$C_D = 0.337078$, $C_L = 0.07400$ (using 500 quadrature points),

$C_D = 0.337064$, $C_L = 0.07398$ (using 1100 quadrature points).

The precision depends on the number of quadrature points as it is the case for the inclined plate.

5.1.4. Circular cylinder

We compare our results to those calculated by Birkhoff and Zarantonello, Brodetski, and Schmieden:

$\phi = 55.04°$ (angle of separation)

Brodetski	$C_D = 0.493$,
Brodetski	$C_D = 0.500$ in second approximation,
Birkhoff and Zarantonello	$C_D = 0.499$,
We find	$C_D = 0.4986$.

$\phi = 124.21°$: we find $C_D = 0$ like Birkhoff and Zarantonello.

5.1.5. Convex and concave circular arcs

In Table 2 we have tabulated the angle of separation, ϕ; the value of C_D given by Birkhoff and Zarantonello, C_D B-*Z*; and our results, C_D Helm. Our program reproduces all the published values except the first one. We cannot explain this difference except by a misprint in [2].

5.1.6. Comparison with experiments

To show that the method described in this paper works for an arbitrary obstacle, we will now present two new Helmholtz flow calculations and compare them with experimental results.

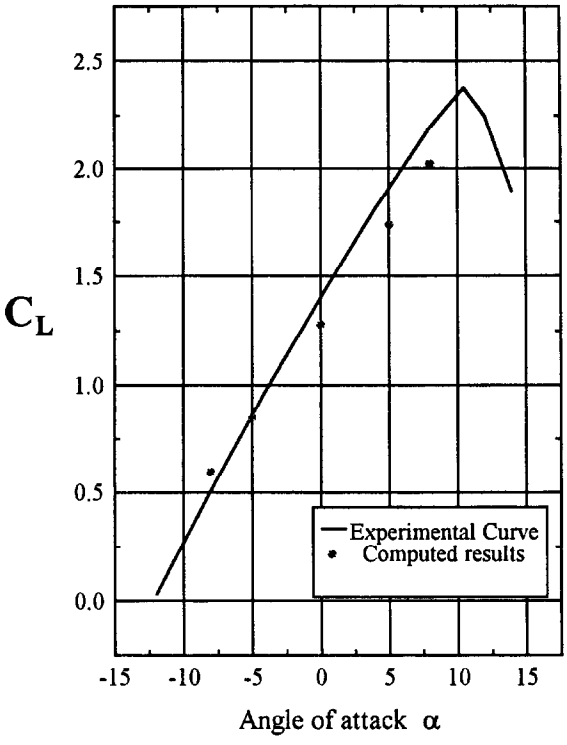

Fig. 6.

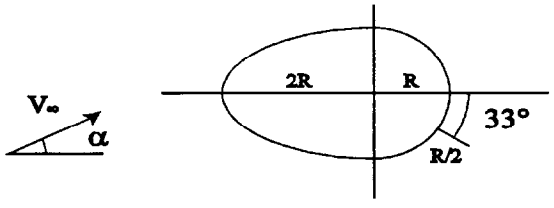

Fig. 7.

The first is a NACA 0012 wing section with a 0.2 chord simulated split flap deflected at 60°. The section lift coefficient is given by Abbott and Von Doenhoff [1], while we calculate C_L when the separation points are placed at the flap extremity and trailing edge. Fig. 6 shows as good an agreement with experimental results as Joukowsky's method in the classical theory of wing sections.

The second calculation is of a thick wing section with boundary layer suction as is used in the Cousteau–Malavard sail of windsail ships. Its surface section consists of a half ellipse upstream and a semi-circle with a flap downstream (Fig. 7). As the boundary layer suction prevents us from

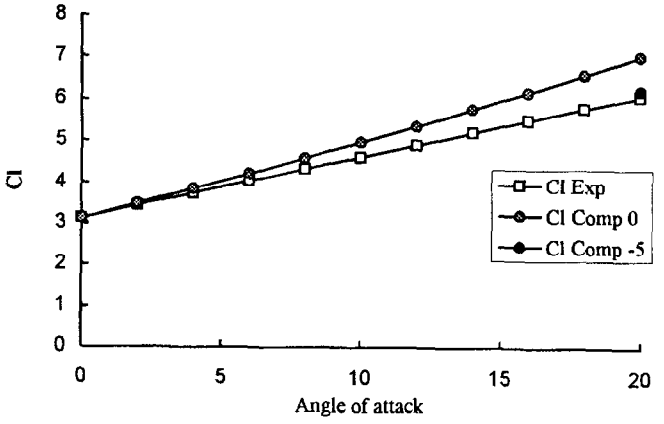

Fig. 8.

-1,2: difference between the jet axis level and the middle plate level [2.5] :h∞ /L

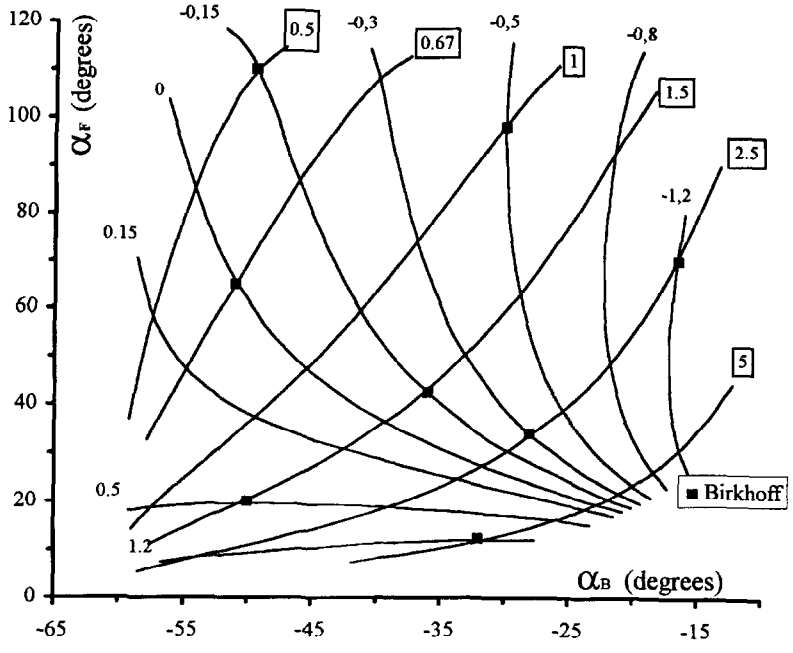

Fig. 9.

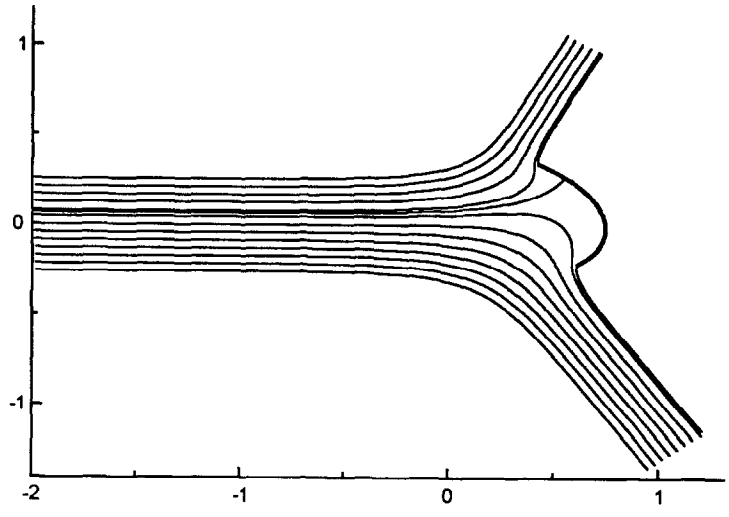

(a)

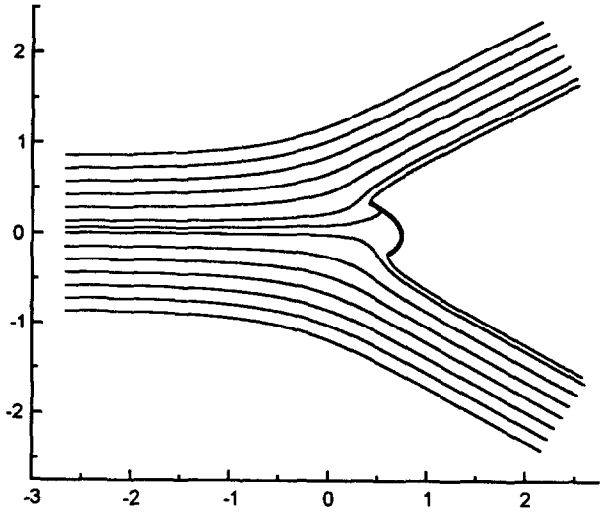

(b)

Fig. 10.

knowing ϕ, we give it a value such that, when α is zero, the C_L we calculate is equal to the experimental one. Then we assume that the separation point is specified. The results are presented in Fig. 8. When α is 20°, C_L is computed as ϕ decreases 5°, because prescribing the separation point is not realistic as the angle α increases. This agrees better with experimental results [4].

The results shown in Figs. 6 and 8 allow us to say that Helmholtz's wake model, in spite of its simplicity, can predict C_L accurately.

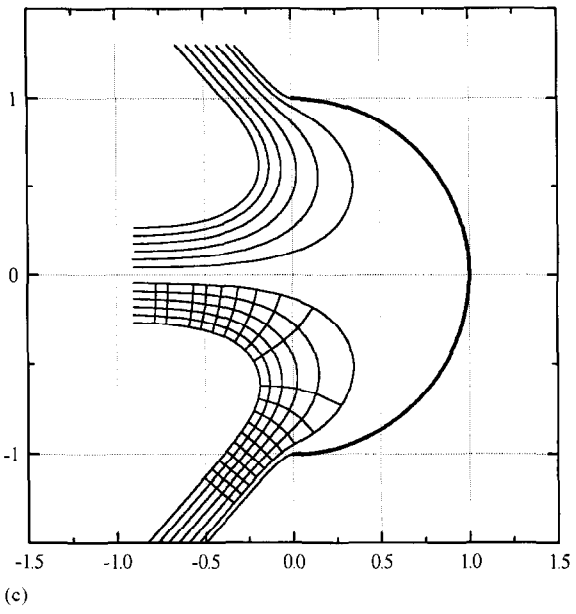

Fig. 10. Continued

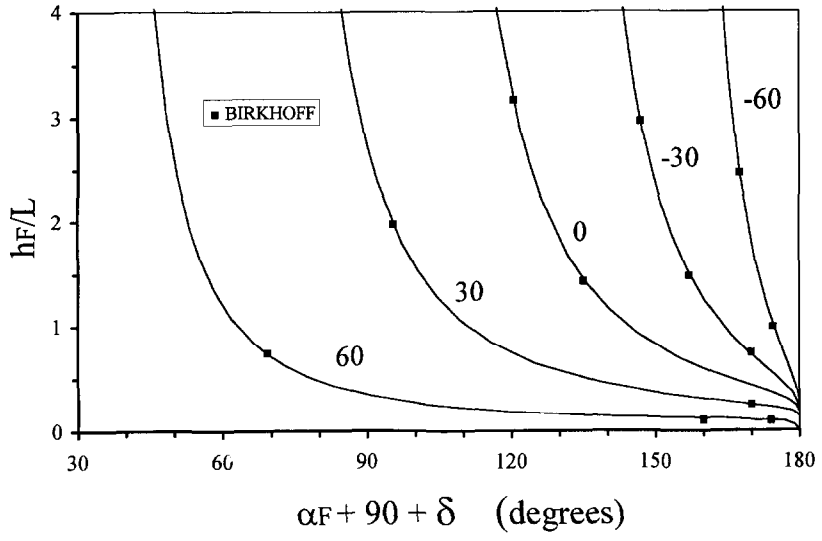

Fig. 11.

5.2. *Jet impinging an obstacle*

As we do not know of any results for a jet flowing over a curved wall, we tested our method with the case of a jet divided by a flat plate, because Birkhoff and Zarantonello (see [2]) published some

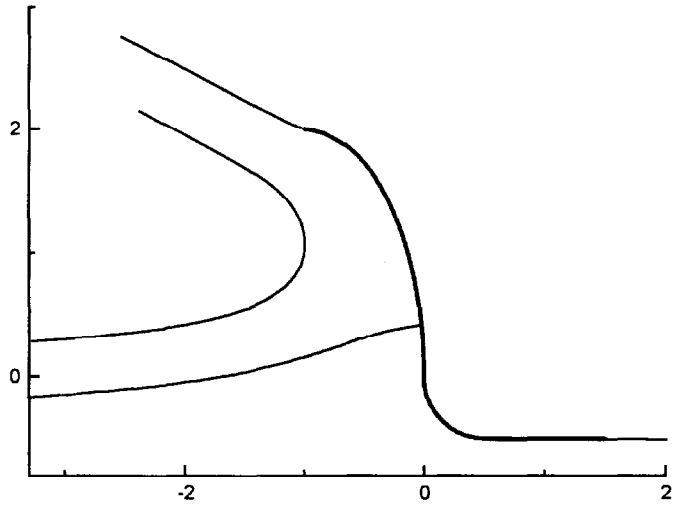

Fig. 12.

results for such a plate inclined at an angle 60°. They present values α_B and α_F, given the plate length L and the position of the obstacle with respect to the jet axis. To test our jet program with the flat plate inclined at different angles, we wrote another program that solves this problem using the log-hodograph domain (Kirchhoff's method) instead of the Schwarz–Villat's formula. The values α_B and α_F that our two programs compute are exactly the same, and they agree with the published values of Fig. 9. The only limitation of this procedure is a sort of crowding which occurs when h_B (or h_F) becomes small compared with L, so that B (or F) approaches -1 (or $+1$) in the ζ-plane.

We will now present some new flow calculations of our own. Fig. 10 shows the flow over an arc of ellipse with a system of streamlines for different widths.

5.3. *Planing on a free surface*

To solve the problem of a curved planing surface, Weinig and Franke (see [7]) used a method that was interesting, but yielded only approximate results, since the shape of the plate is characterized by the two angles that the contour makes with the chord at the leading and trailing edges, and by the angle that the chord makes with the x-axis. The only published results (see [2]) are for a flat plate inclined at various angles. So to test our third program, we compare its results to the published ones. Fig. 11 shows good agreement between these. As in the preceding section, we wrote a secondary program which treats the case of straight obstacles using the log-hodograph domain, and we see that it gives exactly the same results.

As in the jet, a crowding appears as F approaches $+1$ in the ζ-plane.

To show the ability of our program, consider a geometry resembling the bow of a ship (two parts of an ellipse). Fig. 12 represents the obstacle and the free streamlines.

6. Conclusion

We think that our first program, on the basis of its tests, can reliably compute infinite flow over an arbitrary obstacle. When the obstacle divides a jet, or when the obstacle is a planing surface, we have presented only a few comparisons because few are available in the literature. But from the agreements we obtain, we believe that our jet program and planing surface program can also compute these flows for any wetted wall geometry. In this manner, we demonstrate that our method can calculate velocity and pressure fields, C_D and C_L values, streamlines and free streamlines for unbounded flows, ocean and jet flows past any given obstacle. The only limitation is classical crowding, well-known in conformal mapping.

Now one may think that this is an old problem, and that Computational Fluid Dynamics is the only way to solve it nowadays. The panel method has two major advantages over classical two-dimensional flow theory: (i) it is easier to consider several bodies and, of course, (ii) it is the only way to deal with a three-dimensional pattern. However, the singularity method cannot integrate an infinite wake behind an arc. In order to know how far behind the obstacle the wake singularity line should be extended, a comparison with our model has been performed for the simple case of an arc. To obtain the same pressure distribution as computed by our method, we need to take into account more than 100 000 chord lengths with a singularity model, plus an asymptotic behavior of the streamlines [2, 11]. This shows that for multi-elements the panel method should be used, but for a 2D single element survey our method is easier and faster.

This method has also been applied to jets issuing from nozzles of arbitrary shape, yielding good results which will be published later.

Note that C_D can be predicted by a similar method using a different pressure in the wake. The Riemann–Hilbert problem then has to be solved. This is presented in Legallais's thesis [10] and in papers to be published.

References

[1] Abbott and A.E. Von Doenhoff, *Theory of Wing Section* (Dover, New York, 1958).
[2] G. Birkhoff and E.H. Zarantonello, *Jets, Wakes, and Cavities* (Academic press, New York, 1957).
[3] M. Brillouin, Les surfaces de glissement de Helmholtz et la resistance des fluides, *Ann. Chim. Phys.* **23** (1911).
[4] A. Daif and M. Mudry, L'aérodynamique des profils épais aspirés, *7eme congrès français de mécanique* (1985).
[5] B. Demtchenko, sur la formule de H. Villat résolvant le problème de Dirichlet dans un anneau circulaire, *J. de Math. Pures Appl.* Tome **X** (1931).
[6] A.R. Elcrat and L.N. Trefethen, Classical free streamline flow over a polygonal obstacle, *J. Comput. Appl. Math.* **14** (1986).
[7] M.I. Gurevich, *The Theory of Jet in an Ideal Fluid* (Pergamon Press, Oxford, 1966).
[8] J. Hureau, La transformation conforme et l'étude numérique d'écoulements stationnaires ou instationnaires autour d'obstacles avec sillage, Thèse Orléans, 1988.
[9] C. Jacob, *Introduction Mathématique à la mécanique des Fluides* (Gauthier-Villars, Paris, 1959).
[10] Ph. Legallais, Le problème mixte et la modélisation d'écoulements autour d'obstacles avec sillage, Thèse Orleans, 1994.
[11] Ph. Legallais and J. Hureau, Singularity method applied to the classical Helmholtz flow coupling procedure with boundary layer calculation, *J. Phys. III France* **4** (1994).

[12] T. Levi-Civita, Scie e leggi di resistenzia, *Rendiconti del circolo Mathematico di Palermo* Tome **23** (1907).
[13] J. Leray, Les problèmes de représentation conforme d'Helmholtz, théories des sillages et des proues, *Comentaru Mathematici Helvetici* Tome **8** (1935–36).
[14] D. Riabouchinsky, Recherches d'hydrodynamique, Thèse, Paris, 1922.
[15] H. Villat, Sur la resistance des fluides, Thèse, Paris, 1911; *Leçons sur l'hydrodynamique* (Gauthier-Villars, Paris, 1929).
[16] T.Y. Wu, Inviscid cavity and wake flows, in: M. Holt, Ed. *Basic Developments in Fluid Dynamics* (Academic Press, New York, 1968).